JOURNAL OF CATALYSIS 81, 77–94 (1983)

Influence of Ensemble Size on CO Chemisorption and Catalytic *n*-Hexane Conversion by Au–Pt(111) Bimetallic Single-Crystal Surfaces

J. W. A. SACHTLER AND G. A. SOMORJAI

Materials and Molecular Research Division, Lawrence Berkeley Laboratory, and Department of Chemistry, University of California, Berkeley, California 94720

Received July 2, 1982; revised November 30, 1982

Epitaxial Au layers were prepared by vapor deposition of Au on a Pt(111) single-crystal surface. Surface alloys were formed by heating the Pt(111) crystal that was covered with a Au multilayer. The surfaces were characterized with Auger electron spectroscopy (AES), low-energy electron diffraction (LEED), and temperature-programmed desorption (TPD) of CO. LEED showed that both gold overlayers and Pt–Au alloy surfaces were well ordered and had (1 × 1) surface structures. The temperature at the maximum of the TPD spectrum of CO was found to be sensitive to the distribution of Pt atoms in the surface. As a result, epitaxial surfaces were shown to have large Pt ensembles while much smaller ensembles were predominant on alloy surfaces. With TPD of CO it could also be demonstrated that the ligand effect of alloying is absent for CO adsorbed on these alloy surfaces. The differences in ensemble size were found to have profound effects on the skeletal reactions of *n*-hexane. This reaction was carried out *in situ* with 26.7 mbar (20 Torr) *n*-hexane in 267 mbar (200 Torr) hydrogen at 573 K, by utilizing a sample isolation cell. Surface alloys were found to be more active than pure Pt(111). Large increases in the isomerization rate of *n*-hexane and simultaneous exponential decreases of hydrogenolysis and aromatization rates with gold concentration led to high selectivity for isomerization. These effects are caused by changes in the bonding of organic molecules that are induced by structural alterations of the Pt(111) single-crystal surface. Epitaxial gold layers decreased the activity of the Pt(111) surface in proportion to the gold coverage because of the reduction of the available platinum surface area, without substantial selectivity changes.

1. INTRODUCTION

As catalysts for hydrocarbon reactions, alloys of metals have received much attention (*1*). Multicomponent systems may show improved activity, selectivity, and stability. The two concepts that are used most widely to explain the altered catalytic properties are the "ensemble size" or "structural" and the "ligand" or "electronic" effects (*2*).

Upon alloying of, e.g., platinum with gold the concentrations of the various platinum surface sites, which consist of four, three, or two in-plane nearest neighbors, or just single Pt atoms are altered. As gold substitutes for Pt the concentration of the higher-coordination-number, fourfold and threefold sites that make up the large ensembles decreases more rapidly than the concentration of the low-coordination-number (e.g., twofold, single atom), small ensemble sites.

As a result, reactions that proceed through intermediates that are bound to many adjacent Pt atoms will be inhibited more strongly by alloying than reactions that require only small ensembles. The electronic effects are due to charge transfer from one of the alloy components to the other at a given surface site, which markedly alters the chemical bonding of reactants and reaction intermediates at that site leading to modified catalytic activity and selectivity. Although the two effects are not likely to be separable unambiguously, in the absence of large charge transfer from one of the alloy constituents to the other at a given

0021-9517/83 $3.00

surface site the structural effects may predominate. For the Pd–Ag system strong evidence for the predominance of the structural effect was obtained from an infrared spectroscopy investigation of chemisorbed CO (*3*). It was found that upon alloying with Ag the absorption band for CO that was bound to a multiplet of Pd atoms decreased more rapidly than the band for CO adsorbed on top of a single Pd atom. Temperature-programmed desorption (TPD) of hydrogen from Pt–Au alloy surfaces (*4*) did not show a shift of desorption peak temperatures which argues against a significant ligand effect for this system.

However, recent studies of the coadsorption of potassium and CO on platinum indicate that the large charge transfer from K to Pt increases the binding energy of the Pt–CO bond by 50 kJ/mole and also results in the preferential population of bridge sites while CO prefers the top sites in the absence of K. This then, would be an example of an electronic effect that influences the bonding geometry as well (*5*).

In order to explore the molecular basis of the effects of alloying on the catalytic activity we carried out reaction rate studies on well-characterized single-crystal surfaces with known atomic structure and composition. We report here studies of the Pt–Au system. Gold was evaporated onto the (111) crystal face of platinum to form either an epitaxial overlayer or an alloy system. The system was characterized by low-energy electron diffraction (LEED) and Auger electron spectroscopy (AES). Temperature-programmed desorption (TPD) of carbon monoxide was also carried out as a function of gold surface concentration as the CO desorption was found to be sensitive to the surface structure of the Pt(111)–Au system. Catalytic studies were carried out using *n*-hexane, which undergoes several different reactions over platinum: dehydrogenation, isomerization, aromatization, C_5-cyclization, and hydrogenolysis. The experiments were carried out in an ultrahigh-vacuum (UHV) apparatus equipped with a sample isolation cell. In this way, surfaces could be prepared and characterized under UHV conditions with subsequent reaction studies *in situ* at pressures of the order of 1 bar. The bimetallic surfaces were prepared by vapor deposition of Au onto the Pt(111) substrate, in some cases followed by a high-temperature treatment.

It was found that gold overlayers deposited at 300 K uniformly covered the various platinum surface sites without altering their relative concentrations. As gold was allowed to diffuse into the Pt surface by high-temperature annealing to form an alloy, the large Pt ensembles were drastically reduced with a profound effect on the catalytic properties. The surfaces with only small Pt ensembles were more active than pure platinum and had a high selectivity for isomerization, while surfaces with unaltered site distribution behaved as pure Pt(111) with a reduced surface area. The ligand or electronic effect was shown to be insignificant for the Au–Pt(111) system studied here as could be judged by studies of the chemisorption of CO. However, alteration of the Pt(111) surface structure by alloying changed the bonding of organic molecules, and markedly altered the activity and the selectivity of the catalyst.

2. EXPERIMENTAL

2.1. Apparatus

The experiments were carried out in an UHV system equipped with a sample isolation cell to permit *in situ* reaction studies at pressures of up to 1 bar.

Surface characterization was accomplished with four-grid LEED optics that were also used to collect and energy-analyze the Auger electrons which were generated by irradiating the sample with a separate electron gun. A quadrupole mass spectrometer was used for TPD measurements.

The bimetallic surfaces were prepared by vapor deposition of Au onto a Pt(111) single-crystal surface. The effusive-type gold

source was located in a separate, differentially pumped chamber. The evaporation geometry was the same as that in earlier studies (*6*).

The platinum single crystal was spotwelded to very short pieces of 0.5-mm Pt wire spotwelded to 0.8-mm Au wires which in turn were pressed inside matching holes of the Cu feedthroughs. This arrangement is shown in Ref. (*7*) but thinner mounting wires had to be used here. Very even heating without hot spots was assured this way. In order to shorten cooling times after annealing or TPD measurements, the crystal was cooled through the electrical leads by immersing copper bars mounted on the electrical feedthroughs in liquid nitrogen. This also lowered the adsorption temperatures to 250–270 K. The crystal temperature was measured with a Chromel–Alumel thermocouple spotwelded to its edge.

Details of the sample isolation cell are described in Ref. (*8*). Briefly, the crystal was mounted as described from feedthroughs in a small disk that itself was attached to the manipulator. By raising the movable part of the isolation cell against this disk, the single crystal would become enclosed in a small volume that was sealed from the surrounding UHV. In this apparatus a Viton O-ring was used instead of a gold gasket as in Ref. (*8*). Reaction studies could then be performed by passing reactants through this volume and heating the crystal to reaction temperature. The gases were circulated with a Teflon gear pump and samples were taken with a gas sampling valve and analyzed by a gas chromatograph with a flame ionization detector. The system operated this way as a well-stirred batch reactor with a volume of 0.165 liter.

2.2. *Materials*

The Pt(111) single crystal was prepared by spark erosion of a thin wafer from a high-purity single-crystal rod (within 1° of the (111) orientation as determined by Laue back-reflection X-ray diffraction). This wafer was polished mechanically on both sides and etched very briefly in aqua regia before mounting in the vacuum chamber. The hydrocarbons used in these experiments were *n*-hexane (obtained from Phillips Petroleum Co.) and *trans*-hexene-2 (obtained from Aldrich Co.). The purity of the *n*-hexane was found to be 99.95 mole%, by gas chromatographic analysis, with predominantly methylcyclopentane and also some benzene and 3-methylpentane as contaminants. The purity of the *trans*-hexene-2 was found to be 99.9 mole% with pentane-2, *cis*-hexene-2, and 2- and 3-methylpentane as major impurities. The hydrocarbons were degassed by repeated freeze–pump–thaw cycles. The high-purity hydrogen obtained from the Lawrence Berkeley Laboratory was passed through a molecular sieve trap before use.

2.3. *Procedures*

After more severe treatments to remove impurities that were initially present in the new single crystal, the following cleaning procedure was routinely used. First the front and back surfaces were argon ion-bombarded (6.7×10^{-5} mbar (5×10^{-5} Torr), 1-keV ions) for 30 min each, at 295 K. In this way the surface region from the previous experiment was completely removed, preventing the accumulation of Au in the bulk of the Pt crystal. After annealing for 15 min at 1250 K residual carbon was removed in 6.7×10^{-7} mbar (5×10^{-7} Torr) O_2 at 1150 K for 40 sec or less, followed by desorption of any remaining oxygen at 1250 K for 3 min. Then the crystal was cooled and surface cleanliness was checked with AES. If necessary, the oxygen treatment was repeated. The resulting surfaces were clean according to AES and produced LEED patterns with sharp spots. In order to produce an epitaxial surface, gold was deposited in equal amounts onto each crystal face, at 295 K. The accumulation of Au was monitored with AES.

When a surface alloy had to be studied, the clean Pt(111) surface was additionally

characterized by a TPD spectrum of CO, after saturation exposure of 36 L (1 L = 1.3 $\times 10^{-6}$ mbar sec (1×10^{-6} Torr sec)) at 250–270 K. Then three to four monolayers of gold were deposited on each crystal face followed by a thermal treatment consisting of one or more flashes to 1100–1250 K to cause interdiffusion of the Au and Pt. The decrease of the gold surface concentration was followed by AES and after cooling to 250–270 K a TPD spectrum of CO was recorded, after 36-L exposure.

Next the sample isolation cell was closed and 26.7 mbar *n*-hexane was introduced, followed by 267 mbar hydrogen. After circulating the gases for 10 or 20 min, respectively, with the crystal at room temperature, two samples were taken to verify the gas composition and the absence of background activity. Three minutes after the reaction was started by heating the crystal to the reaction temperature of 573 K, another sample was taken followed by more at 10-min intervals, for the duration of the reaction. After the reaction time of 3 h the crystal was cooled in the reaction mixture and the reactor was evacuated. Finally, the cell was opened and the surface reexamined. As the sample isolation cell was set up as a batch reactor, kinetic data were obtained in the form of product accumulation curves. Using the surface area of the Pt(111) crystal that was measured geometrically (0.7 cm^2) the amounts of product were calculated as molecules formed per surface atom. Unless otherwise specified, data in this paper were calculated per total number of surface atoms, Pt + Au. Initial rates were obtained by graphically determining the initial slopes of accumulation curves. The fission parameter, M_f, characterizing the hydrogenolysis product distribution, was calculated in the usual way (*9*). The amounts of hydrogenolysis products were calculated as the number of hexane (or hexene) molecules consumed, except for the hydrogenolysis product distributions where molefractions were used. The experiments in which aromatization was studied were carried out separately as a different column had to be used in the gas chromatograph for the separation of benzene.

The TPD spectra were measured by the quadrupole mass spectrometer, upon heating the crystal at a rate of 68 K sec^{-1}. During CO adsorption, the crystal temperature was 250–270 K. Separation of the overlapping Au and Pt Auger transitions, determination of the film growth mechanism of Au deposited on the Pt(111) surface, and calibration of the gold coverages were carried out according to the procedures described in Ref. (*6*) for Au on Pt(100).

3. RESULTS

3.1. Surface Characterization with AES and LEED

3.1-1. Epitaxial Au layers on Pt(111). As has been discussed in the literature (*10*), and studied in detail with the Au on Pt(100) and Pt on Au(100) systems (*6*), AES can be used to determine the growth mechanism of the metal that is deposited onto the surface of another metal. In order to obtain this information, an Auger signal versus time of deposition (ASt) plot has to be generated. The various growth mechanisms show characteristic features in their ASt plots through which they may be identified. With the current system this analysis is complicated by the overlap of Au and Pt Auger transitions, as is evident from Fig. 1 where Auger spectra are shown recorded after various times of deposition of Au on Pt(111), at 295 K. After applying the peak separation following Ref. (*6*) an ASt plot could be constructed and the result is shown in Fig. 2. It should be noted that under conditions of constant deposition rate as used here, the deposition times are proportional to the Au coverages.

Careful inspection of the data plotted in Fig. 2 reveals three breaks, at deposition times of 13.0, 27.0, and 39.5 min. An observation of multiple breaks at times obeying the ratio 1 : 2 : 3 as expected for a successive completion of three monolayers, indi-

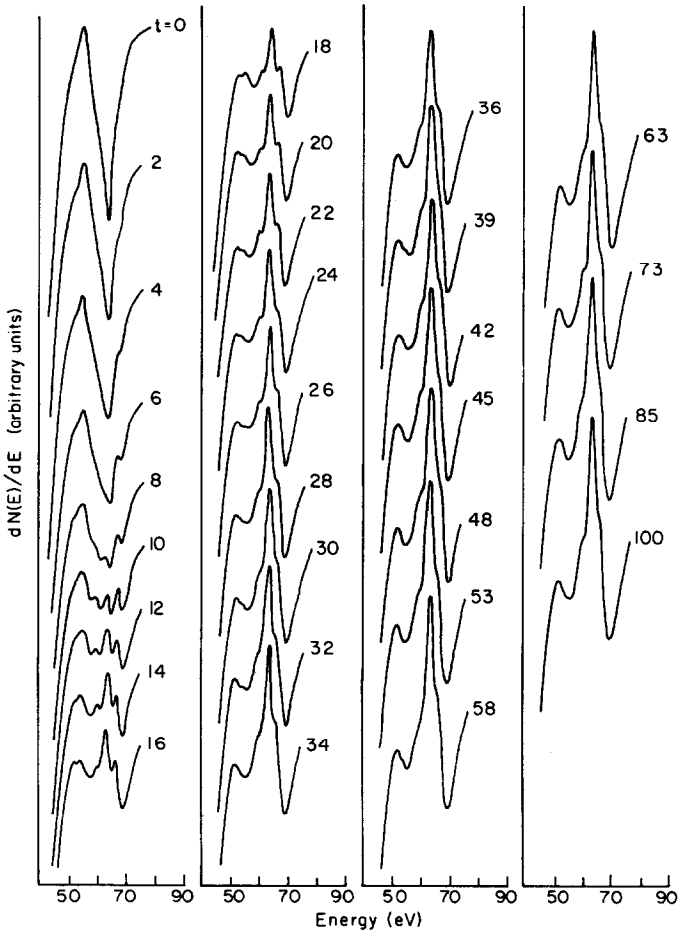

FIG. 1. Auger spectra of Pt(111) covered with various amounts of Au. t indicates deposition time, in minutes, at constant evaporation rate.

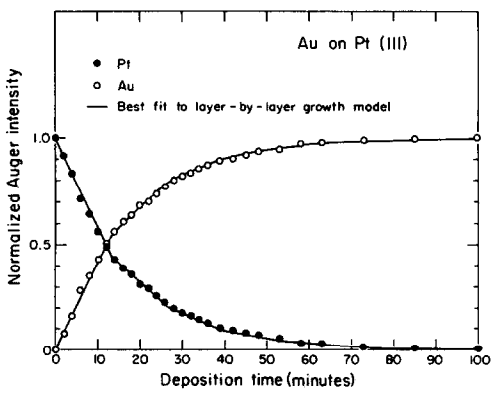

FIG. 2. Auger signal versus time plot of Au on Pt(111).

cates a layer-by-layer (Frank–van der Merwe) growth mechanism. The data in Fig. 2 could also be described numerically with the layer-by-layer growth mechanism using the Gallon model (*11*) and the calculated curve that gave the best fit is shown by the solid lines in Fig. 2. Using the monolayer deposition time of 13.2 min obtained from the positions of the breaks, optimization of the fit gave a normalized monolayer Auger intensity $I(1)/I(\infty) = 0.55$ and a variance (sum of squares of the differences between calculated and experimental values) $V = 0.0038$. The parameter $I(1)/I(\infty)$ is related to the mean free path, λ, of the Auger

electrons (*12*) and using an interlayer spacing of 0.226 nm (based on the bulk Pt lattice constant of 0.392 nm (*13*)), a value of λ = 0.38 nm was calculated. It should be noted that the determination of the monolayer deposition time automatically also provides the coverage calibration of the Auger spectra.

LEED observations of these surfaces revealed the following. The clean Pt(111) surface showed the expected hexagonal diffraction pattern. Upon deposition of Au this pattern was always retained. Submonolayer amounts of gold, as well as multilayers, did not lead to any new spots, even after annealing at temperatures as high as 1270 K. The sharpness of the diffraction spots did, however, appear to decrease slightly after several layers of Au had been deposited.

From measurements of spot–spot distances in LEED patterns obtained at different Au coverages, changes in the surface lattice constant have been calculated. The accuracy of these measurements was limited by the sizes of the diffraction spots which were significant compared to the 4% difference in bulk lattice constants of Au and Pt (0.40785 and 0.39239 nm, respectively (*13*)). Within the accuracy of these measurements of about 1% of a lattice constant, a continuous increase of the lattice constant of the clean Pt(111) surface toward that of Au(111) was found, spread out over about five or more monolayers. One monolayer of Au on Pt(111) had the same lattice constant as the substrate, within experimental accuracy, and was clearly contracted as compared with the bulk value.

3.1-2. Surface alloys. AES was used to follow the decrease of the amount of Au at the surface upon annealing but it was not used for quantitative determination of the Au and Pt surface concentrations, as the depth profile of the composition was not known.

LEED observations of a series of alloy surfaces that were generated by heating the Pt(111) single crystal covered with a multilayer Au deposit for various lengths of time to increasing temperatures, showed that in all cases the alloy surfaces were well ordered with the same geometry as the Pt(111) substrate. Extra spots, indicative of reconstruction or of the formation of new surface structures, were not observed.

3.2. Surface Characterization with TPD of CO

3.2-1. Clean Pt(111). A series of TPD spectra recorded after various exposures is shown in Fig. 3. Only one peak is observed with a peak maximum temperature, T_m, that shifts to lower values with increasing exposure. This variation is presented explicitly in Fig. 4. From these values the activation energy for desorption, E_d, can be calculated using Redhead's equation for first-order desorption kinetics (*14*). Assuming a preexponential factor of 10^{13} sec^{-1}, a value of E_d = 116 kJ/mole is obtained after extrapolation to zero coverage. This value

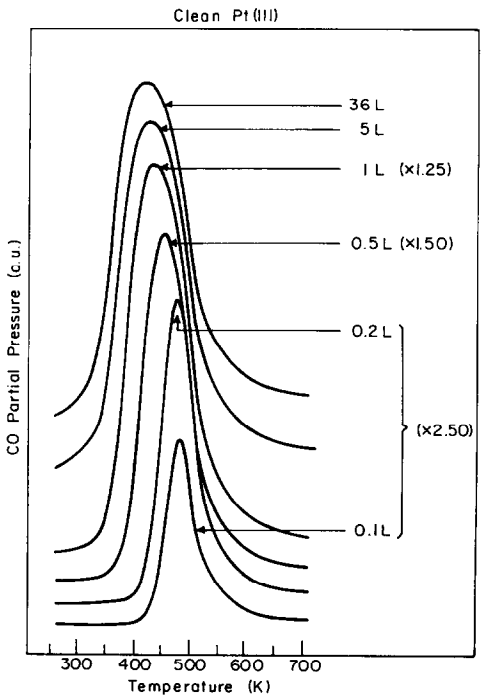

FIG. 3. TPD spectra of CO adsorbed on Pt(111), as a function of exposure.

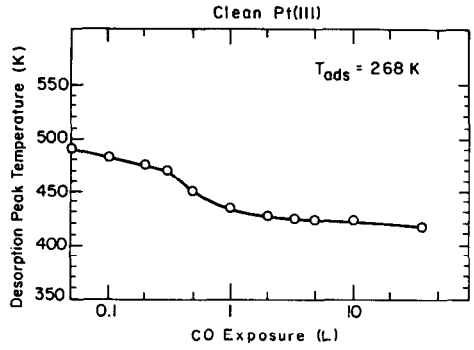

FIG. 4. Variation of the desorption peak temperature with CO exposure. (1 L = 1 Langmuir = 1.3×10^{-6} mbar · sec (1×10^{-6} Torr · sec).)

is in good agreement with literature values of 117 (*15*), 124 (*16*), and 113 kJ/mole (*17*). The decrease of T_m from 490 to 415 K with increasing CO exposure (Fig. 4) can be explained by repulsive interactions between the adsorbed CO molecules because of crowding that increases with increasing coverage and weakens the CO–Pt bonds. Because of this dependence, T_m can be used as a measure of the average CO–CO distance in the adsorbed layer. This interpretation is of importance for the analysis of TPD spectra from the bimetallic surfaces.

3.2-2. Epitaxial Au on Pt(111). Figure 5

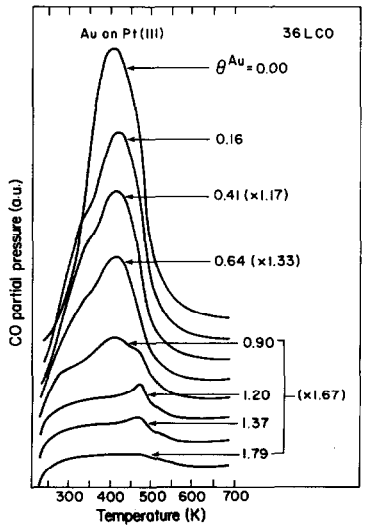

FIG. 5. TPD spectra of CO adsorbed on Pt(111) covered with varying amounts of gold, after constant saturation exposure of 36 L.

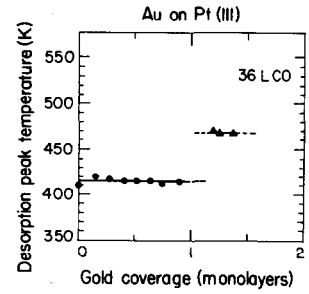

FIG. 6. Variation of the desorption peak temperature, after constant saturation exposure of 36 L, with gold coverage on Pt(111). ●: Pt(111) surface covered with submonolayer amounts of gold. ▲: Pt atoms that diffused through the Au layer, an artifact of these measurements.

shows the TPD spectra of CO from the Pt(111) surface that was covered with various amounts of Au deposited at 295 K. All desorption traces were recorded after 36-L exposures, high enough to saturate the surface with adsorbed CO molecules. There are two major observations: (1) the temperature, T_m, of the maximum rate of desorption does not change with gold coverage and remains the same (415 K) as that obtained on the clean Pt(111) face at high CO coverages. This is shown in Fig. 6. This indicates the presence of *large patches of uncovered Pt(111)* where neighboring CO molecules can exert their repulsive interaction. (2) There is a linear reduction in the amount of CO adsorbed with gold coverage. This is shown in Fig. 7. The position of

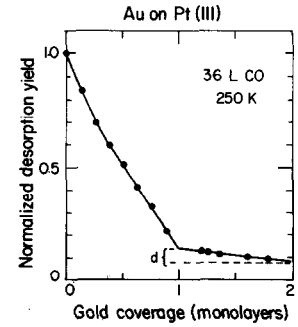

FIG. 7. Variation of the normalized desorption yield, after constant saturation exposure of 36 L, with gold coverage on Pt(111).

the break in Fig. 7 which indicates the completion of the first monolayer is in excellent agreement with the coverage that was determined from the ASt plot.

In a separate experiment it was found that after heating a gold-covered surface to 700 K, the highest temperature of the TPD spectra, a peak at about 470 K was observed. This peak was not present before heating to 700 K. Thus, this apparently new state in Fig. 5 is due to diffusion of substrate Pt atoms through the Au layer at the elevated temperatures of the TPD measurements.

The other new feature of Fig. 5 is a low-temperature shoulder that is not an artifact. It was observed that this shoulder decreased in intensity in a second desorption measurement on the same surface, to which no more Au had been added. At the elevated temperatures of the temperature ramp, faster surface diffusion and aggregation of Au into larger two-dimensional islands would be possible. These larger islands would have a smaller total circumference which would explain the observations if this desorption state is due to CO chemisorbed on Pt atoms next to the step formed by a gold island boundary.

In this paper the amounts of CO desorbed will be presented as normalized yields which are defined as the area under desorption curves divided by the area under the desorption curve for clean Pt(111) after saturation exposure of 36 L. In order to maximize reproducibility a new Pt(111) reference TPD spectrum was measured at the beginning of every experimental sequence.

As TPD of CO is able to detect very small amounts of Pt, this technique was also used to investigate the stability of a gold layer at the reaction temperature of 573 K. The TPD spectrum of the Pt(111) surface covered on each side by 1.2 monolayers of Au only showed the featureless broad peak characteristic of the edges of the crystal. After heating to 573 K for 11.8 h a small alloy desorption peak was found on top of this background desorption. The desorption yield of this peak was only 0.1% of that of clean Pt(111) which demonstrates the high stability of the epitaxial layer at this temperature.

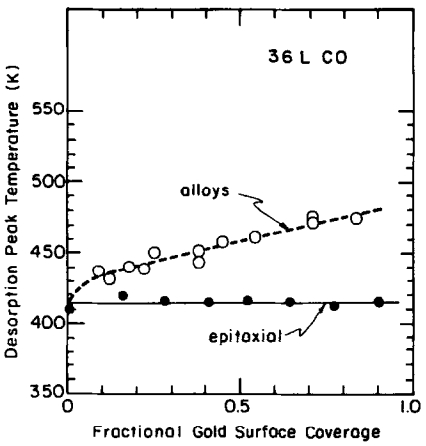

FIG. 8. Variation with surface gold content of the desorption peak temperature, after saturation exposure of 36 L, for epitaxial and alloy surfaces.

3.2-3. Au–Pt(111) surface alloys. When CO was adsorbed to saturation coverage on the Au–Pt(111) alloys the maximum desorption rate occurred at higher temperatures than on the epitaxial Au–Pt(111) surfaces. This is shown, as a function of gold surface concentration, in Fig. 8. On the alloy surface, T_m approaches the value (490 K) that is obtained for the clean Pt(111) surface at low CO coverages when repulsive interactions among the CO molecules do not weaken the CO–Pt bond. Thus, it appears that in the alloy the gold atoms do not permit the crowding of the CO molecules that, therefore, maintain their higher binding energy to the platinum atoms. Apparently gold atoms in the alloy break up the available platinum surface into small ensembles that can no longer adsorb a dense layer of CO molecules in which repulsive interactions lower T_m from 490 to 415 K. Gold alloying has the effect of preventing the crowding of CO molecules by creating small platinum islands that can only be sparsely populated with CO. In conclusion, T_m when determined by CO desorp-

tion after 36-L exposures from the epitaxial gold–Pt(111) and gold alloy–Pt(111) systems reveals that (a) there are only large platinum ensembles present in the surface of the partially gold covered epitaxial system while (b) small platinum ensembles predominate in the surface of the Au–Pt(111) alloy.

As CO selectively chemisorbs on Pt under our conditions, the amount adsorbed was used to determine the surface composition (*18*). Thus, the platinum surface concentration was taken to equal the normalized CO desorption yield after saturation exposure, after correction for edge effects (see Section 3.3-2).

3.2-4. The absence of the ligand effect for CO adsorption in the Au–Pt(111) system. It is possible that upon alloying T_m not only changes due to geometrical separation of the CO molecules, but also because of a change in the intrinsic bonding abilities of a Pt atom when its Pt neighbors are replaced by Au. In order to investigate this effect the surfaces have to be studied under conditions where the influence of CO–CO interactions has been eliminated. One way of doing this is by going to the limit of zero CO coverage. Then, chemisorption bond strengths of a single CO molecule on a clean Pt(111) surface and a single CO adsorbed on a Pt atom that is surrounded by Au neighbors can be compared. (According to the literature, at low coverages CO on Pt(111) is adsorbed in on-top sites (*19*).) The difference in T_m between these two cases will then indicate the importance of the ligand effect. Figure 9 shows the relevant observations. For clean Pt(111) the variation of T_m with CO coverage was obtained by varying the CO exposure. Going to very low exposures, which corresponds to going to the left in Fig. 9, a sudden increase of T_m is observed that cannot be explained by decreasing CO interactions as this effect should level off. The sudden rise is then attributed to imperfections of the single-crystal surface and the crystal edges, that bind CO more strongly than terrace Pt

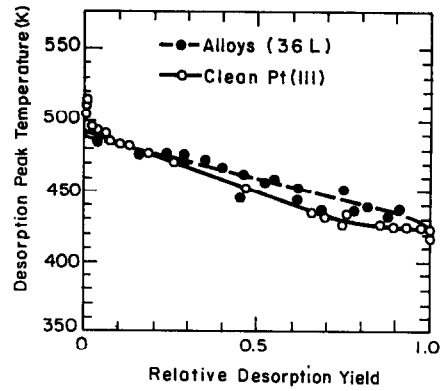

FIG. 9. Variation of the desorption peak temperature with normalized CO desorption yield, for clean Pt(111) and alloy surfaces.

atoms (*20*). At the lowest exposures, only these sites are populated. In order to eliminate this effect the middle range of the data was extrapolated to zero CO coverage. For the alloys, exposures were always at the saturation value of 36 L. Extrapolation of the alloy data to zero yield gives T_m for a single CO adsorbed on a surface platinum atom with only Au neighbors. As Fig. 9 shows the two cases give the same T_m within the experimental error of about 5 K. This error bar of 5 K only corresponds to a difference in adsorption energy of 1.2 kJ/mole which is insignificant compared to the 16.7 kJ/mole coverage-induced variation of the chemisorption bond strength.

3.3. Conversion of n-Hexane

Under the reaction conditions used in this work, *n*-hexane was converted to *cis*- and *trans*-hexene-2, 2- and 3-methylpentane (2-MP, 3-MP), methylcyclopentane (MCP), smaller hydrocarbons ($\Sigma < C_6$), and benzene (BZ). The *cis*- and *trans*-hexene-2 were the only olefins that could be detected. The kinetic data were obtained as product accumulation curves of which two examples are shown in Figs. 10a and b. The kinetics of the hexene-2 formation could not be followed as the first data points were already close to the hexane/hexene equilibrium, particularly in the case of gold-containing surfaces where olefin formation was

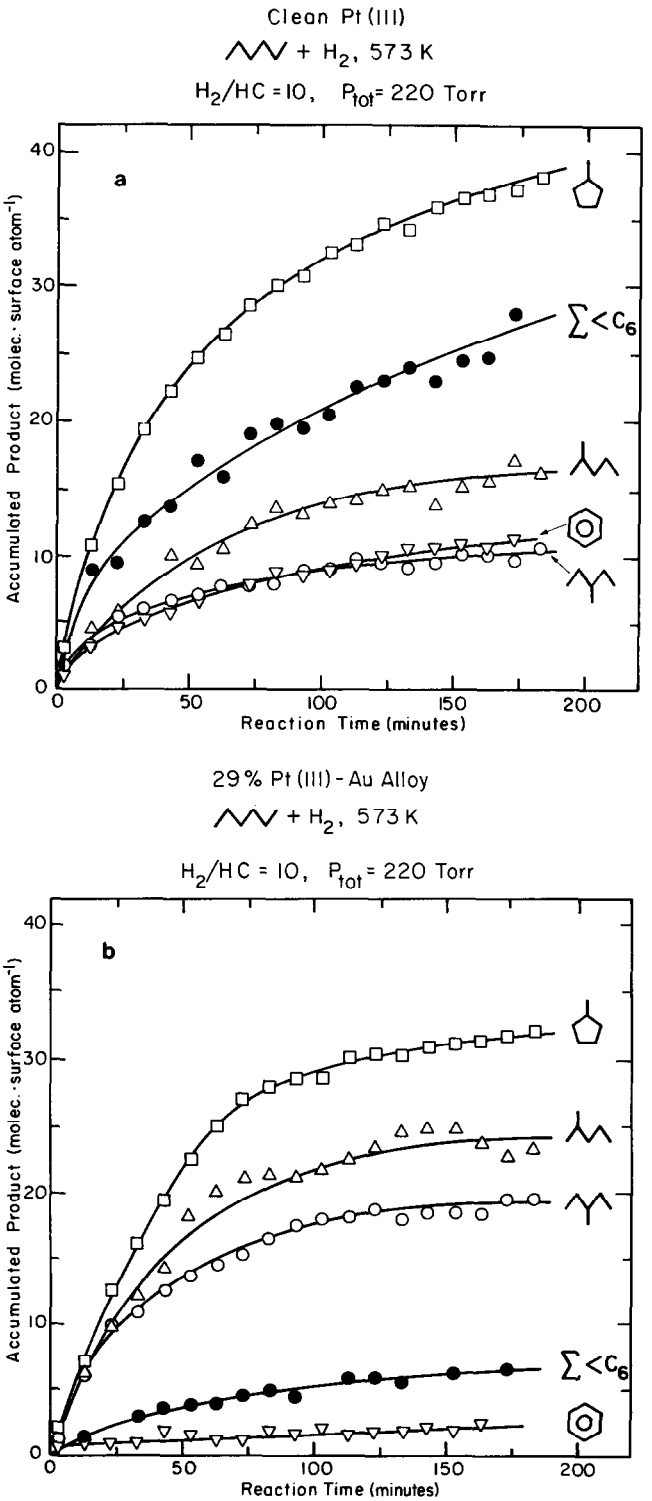

FIG. 10. Product accumulation curves for *n*-hexane reactions. (a) Clean Pt(111) surface. (b) Alloy surface with platinum surface concentration of 29 at.%.

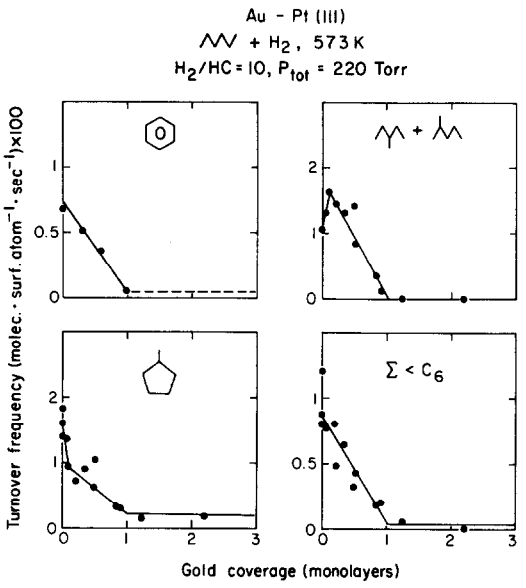

FIG. 11. Gold coverage dependence of the initial formation rates of products from the *n*-hexane reaction catalyzed by the epitaxial surfaces.

enhanced. Initial selectivities were calculated from the initial rates which were determined by graphical determination of the initial slopes of the accumulation curves. As is evident from Fig. 10, steady-state rates were not reached due to self-poisoning. "Integrated" selectivities were calculated from the amounts of products accumulated in 2 h of the reaction.

3.3-1. Epitaxial Au layers on Pt(111). Initial rates of formation of 2- and 3-MP, MCP, $\Sigma < C_6$, and BZ are plotted against gold surface coverage in Fig. 11. All measurements were performed at very low conversion levels (see Fig. 18). It should be emphasized that in this figure, as in Figs. 12, 15, and 18, initial rates have been calculated per total number of surface atoms, i.e., Pt + Au. As it was experimentally not possible to cover the crystal edges with gold, some activity remained at high gold coverages. Thus, a linear decrease of the rate of formation from zero to monolayer Au coverage, followed by a low but constant level of activity indicates that the turnover frequency per *platinum* surface atom is actually constant. As Fig. 11 shows this was the case for aromatization and hydrogenolysis. Isomerization and C_5-cyclization, of which it is known that they may have the same precursor (*21*), showed a different behavior. However, the sum of the latter reaction rates did show the same linear coverage dependence (Fig. 12). This can be understood if at least a part of MCP and 2- and 3-MP was indeed formed through a common intermediate. The linear decrease of the total amount of products and consequently also of the amount of intermediate formed, reflects the decrease of available Pt(111) surface area with increasing Au coverage. Additionally, Au apparently shifted the selectivity of product formation from the intermediate toward isomerization, at the expense of MCP. The selectivities that were calculated from the initial rates, after correction for edge contributions, are shown in Fig. 13.

3.3-2. Separation of face and edge contributions to the total n-hexane conversion and CO desorption. An additional benefit from the study of epitaxial gold layers on a single-crystal surface of an active metal is that face and edge contributions can be sep-

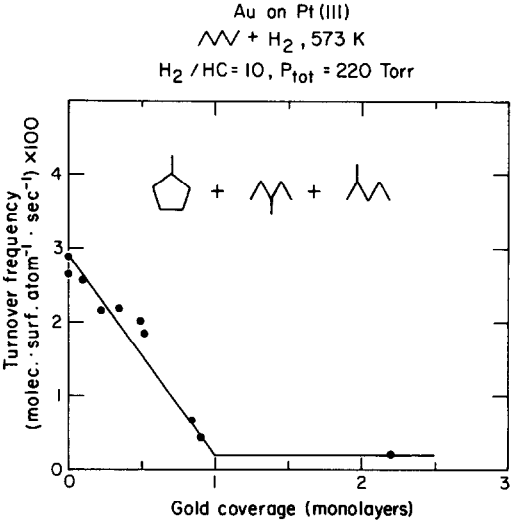

FIG. 12. Sum of rates of formation of methylcyclopentane and 2- and 3-methylpentane as a function of gold coverage.

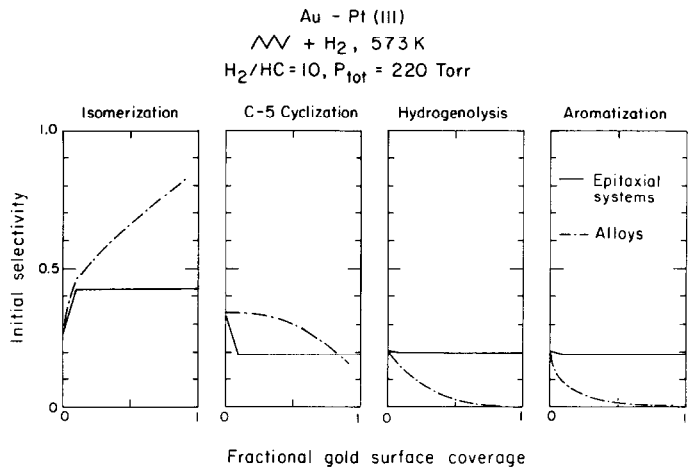

FIG. 13. Initial product selectivities of the *n*-hexane conversion catalyzed by epitaxial and alloy surfaces.

arated. The edges expose a multitude of crystal orientations and often contain impurities in the surface as they are at least partially shadowed during argon ion cleaning, and consequently they may have different properties than the front and back faces of the crystal. Thus, they may perturb reactivity and TPD results. However, when the polished crystal faces are covered by Au, the edges remain uncovered and their activity can thus be identified and used to correct the results. As Fig. 11 shows, the edges are rather unimportant for the results shown there. However, the crystal edges are quite different in their hydrogenolysis product distribution. As is shown in Fig. 14, the edges produce predominantly methane while the clean, well-oriented (111) surfaces also give substantial amounts of propane. Without subtracting the edge contribution, too low a value of the fission parameter, M_f, would have been obtained for the Pt(111) surface.

3.3-3. Au–Pt(111) surface alloys. Figure 15 shows the gold surface concentration dependence of the initial rates of formation of the products from the *n*-hexane reaction, catalyzed by surface alloys. The most strik-

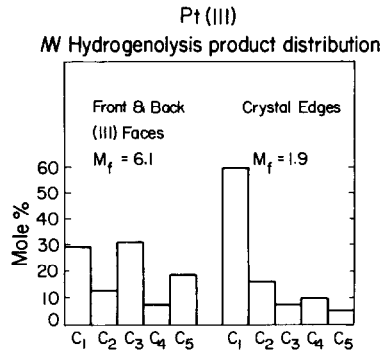

FIG. 14. Hydrogenolysis product distribution for the Pt(111) surface (corrected for edge contributions) and for the crystal edges.

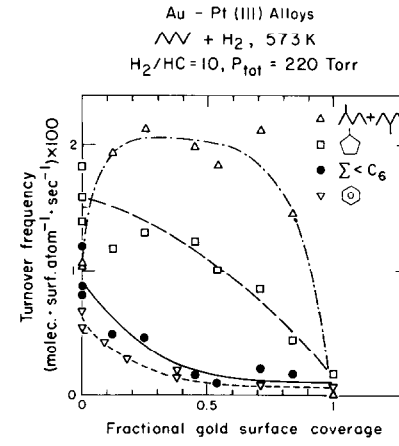

FIG. 15. Gold surface concentration dependence of the initial formation rates of products from the *n*-hexane reaction catalyzed by surface alloys.

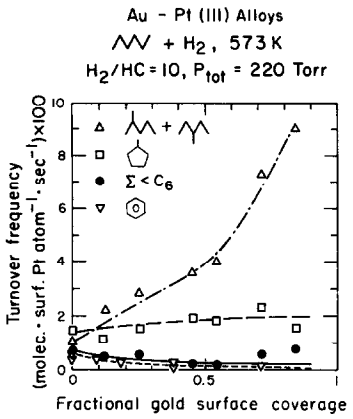

FIG. 16. Variation of reaction rates calculated per *platinum* surface atom, with alloy gold surface concentration.

ing feature is the increase of the isomerization rate, when active Pt atoms are replaced by inactive Au. The increase of the isomerization activity is already seen by comparing Figs. 10a and b where the data are presented in the form of accumulation curves. Aromatization and hydrogenolysis are inhibited by the addition of gold while C_5-cyclization shows a roughly linear decline with gold concentration. In Fig. 16 the same results are shown, but now the rates have been calculated per *Pt* surface atom, after correction for edge contributions. In this case, possible inaccuracies of the determination of the surface composition have been included in the rates, unlike in Fig. 15. Also, the scatter of the data becomes magnified at high gold coverages, in Fig. 16. The addition of gold to Pt(111) as epitaxial islands also caused some enhanced isomerization but the differences between the two types of surfaces are significant as can be seen in Fig. 13. A *major* difference is that the selectivity effects of the epitaxial surfaces were only transient while alloying with Au changed the nature of the surface permanently. This becomes evident from Fig. 17 where the "integrated" selectivities for both systems are plotted against surface gold concentration. Here, the epitaxial Au islands show no modification of the Pt(111) properties while the alloys clearly exhibit enhanced isomerization. Figure 18 demonstrates that not only the integrated selectivities, but also the cumulative activities after 2 h of reaction of the alloys are different from those of the epitaxial surfaces. As the latter behave as pure Pt(111) surfaces with reduced surface area, it is concluded that the alloys are always more active than pure Pt(111) with the same active metal surface area. It should be mentioned, that the Au and Pt surface concentrations were not altered

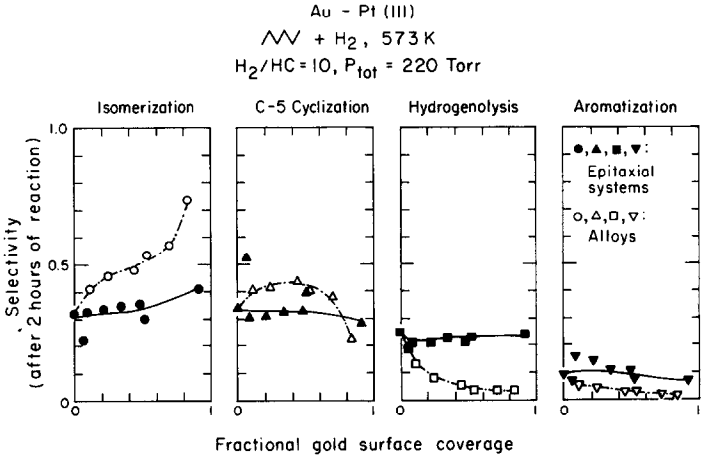

FIG. 17. "Integrated" product selectivities of the *n*-hexane conversion calculated using amounts of product accumulated in 2 h of the reaction.

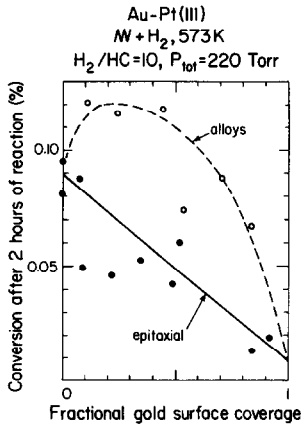

FIG. 18. Conversion of *n*-hexane in 2 h of reaction as a function of surface gold concentration for epitaxial and alloy surfaces.

during the reaction, within the accuracy of AES.

3.3-4. Formation of a carbonaceous overlayer during reaction. During hydrocarbon reactions strongly bound, (partially) dehydrogenated fragments are formed on the catalyst surface. In the apparatus used here, after reaction the cell could be opened and the surface could be examined again with LEED and AES. Because of the UHV environment, only strongly bound species would remain on the surface. LEED observations after reaction did not show a pattern, indicating the absence of an ordered overlayer. AES could be used to determine the amount of carbon on the surface and the results are shown in Fig. 19. Neither these data, nor the LEED observations, were altered by heating the surface under vacuum to 573 K before the surface characterization. An Auger peak intensity ratio of the 272-eV carbon and 237-eV platinum transitions of 3.2 was used to identify one carbon monolayer (*22*), which has been shown to contain two carbon atoms per surface atom (*23*). Since the Au and Pt Auger spectra are very similar and in this energy range practically identical, the same carbon coverage calibration was used for Au-containing surfaces. As the data in Fig. 19 are quite scattered, a gray-shaded area is used to indicate the range that covers most of the results for the epitaxial surfaces. It should be noted that even on Au *multilayers* which are also plotted in the figure (at a fractional gold surface coverage of unity), carbon deposition occurred. Separate experiments of the same reaction under the same reaction conditions with a pure Au single crystal proved that carbon deposition on gold does indeed occur. The alloy values seem to be lower than the epitaxial ones, but the significance of this difference is uncertain.

3.4. Reproducibility and Reliability of the Measurements

The experiments described in this paper were all carried out on the same Pt(111) single crystal. The agreement between our TPD data and those reported in the literature (*15–17*) was excellent. The reproducibility of the Au coverage determination from the Auger spectra (after normalizing the signal intensities using the spectrum of the clean Pt(111) surface measured at the beginning of the experimental sequence) is 5–10% for coverages below two Au monolayers. Above two monolayers, the Auger spectra became increasingly less sensitive to the Au coverage until a constant, pure Au, spectrum was obtained after about five monolayers. The reproducibility of the

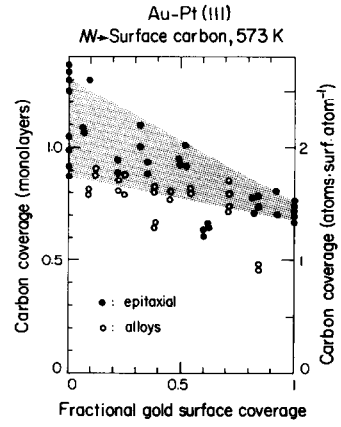

FIG. 19. Amounts of strongly bound carbon deposited on the epitaxial and alloy surfaces in 3 h of reaction.

TPD results is about 5 K for T_m, and 5–10% for the normalized desorption yields. The excellent agreement between the Auger and the TPD-derived coverage data (Fig. 7) certainly indicates a high reliability for these measurements. The data shown in Fig. 9 have been obtained from many different experiments, including the characterization of the alloy surfaces that were actually used for the catalytic reaction studies.

Concerning the catalytic reactions, it is difficult to analyze all the factors that cause the scatter of the kinetic data. The reproducibility has to be judged from the scatter of the measured rates. Generally, they are reproducible to better than 15%, although sometimes larger deviations are found, as is evident from the figures in this paper. The scatter in the initial reaction rates is enhanced by the sensitivity of the graphical differentiation of the accumulation curves to the uncertainty of the first datapoints. Attempts to fit the accumulation curves to a mathematical expression, which would then allow calculation of the derivatives, were unsuccessful.

The reproducibility of the measurement of carbon coverages using AES appears to be about 20%.

4. DISCUSSION

4.1. The Presence of Small Pt Clusters in the Pt–Au Alloy Surfaces and of Large Pt Clusters in the Pt–Au Overlayer Surfaces

Temperature-programmed desorption of CO provides important information on the nature of the bimetallic surfaces. The temperature T_m has been found to be sensitive to the distribution of platinum atoms in the surface. This interpretation is based on the variation of T_m with CO coverage on the clean Pt(111) surface. With increasing coverage the distances between adsorbed CO molecules decrease, increasing their mutual repulsive interactions and thus lowering the activation energy for desorption.

When the Pt atoms in the surface remain as fairly large contiguous arrays (large ensembles) CO molecules can still be packed as closely as is permitted by the repulsive interactions, and these large ensembles will behave as clean Pt(111) surfaces. This is the case for epitaxial gold layers on top of platinum. However, when the Pt atoms are randomly distributed in the surface as in the Au–Pt alloys this will no longer be the case. Then, with increasing gold concentration the probability of finding large ensembles will decrease more rapidly than the chance of finding small ensembles. Consequently, with increasing Au concentration the average ensemble size will decrease. Although a distribution of ensemble sizes exists at any given surface composition, this discussion will be held in terms of average ensemble size as this is the quantity that is reflected by the experimentally obtained parameter T_m. As the ensembles become smaller, fewer CO molecules will be adsorbed per ensemble, reducing on the average the number of neighbors that every CO molecule can interact with. The interactions with CO molecules on other ensembles will be weaker since the ensembles are spatially separated by Au. Thus, the adsorption energy of CO will increase with increasing Au surface concentration in the case of the Au–Pt alloy where Au and Pt are randomly distributed in the surface.

A new desorption state with a lower binding energy was observed on the epitaxial surfaces. This state was attributed to the edges of the Au islands and may be caused by steric hindrance by a gold step on the bonding of CO to an adjacent Pt atom. However, this state is much less populated than the state corresponding to the main peak and does not affect T_m.

The picture of the epitaxial surfaces is one of two-dimensional Au islands that leave large patches of platinum uncovered which retain their Pt(111) character. Only adsorption on Pt atoms adjacent to the edges of a Au island is somewhat perturbed.

LEED observations of both the alloy and

the epitaxial Pt–Au surfaces showed that they were all well ordered and had (1 × 1) surface structures. Thus, they did indeed represent (111)-oriented surfaces.

4.2. *n-Hexane Conversion over Pt–Au Alloy and Pt–Au Overlayer Surfaces*

The results of the *n*-hexane conversion demonstrate that the two types of surfaces have different catalytic properties and we ascribe this to the differences in ensemble size. Van Schaik *et al.* (*24*) reported that upon alloying platinum with gold, the selectivity for hydrogenolysis declined rapidly, dehydrocyclization showed a maximum and then decreased, while the selectivity for isomerization increased. These experiments were carried out in a flow reactor at a total pressure of 1 bar, using SiO_2-supported particles. The good agreement of these findings with the "integrated" selectivities obtained in our work (Fig. 17) supports the expectation that our results can be compared with results obtained under steady-state conditions using supported Au–Pt alloy catalysts.

There is, however, one major difference between results from this work and those in Ref. (*24*). The Au–Pt alloys in this work having small platinum clusters were always more active than surfaces where the same amount of Pt was arranged in larger ensembles (Fig. 18). In the study reported by Van Schaik *et al.* all reaction rates involving C–C bond rearrangements were found to always decrease with increasing concentration of the Ib metal, Au. Selectivity changes occurred because some of the reactions were inhibited more strongly than other reactions.

Sinfelt *et al.* (*25*) have reported similar results, viz., a suppression of hydrogenolysis and an enhancement of isomerization, for the *n*-heptane conversion catalyzed by supported Pd–Au alloys. Interestingly, they did find that the alloys were more active than pure Pd, due to enhanced isomerization. It should be noted that they used an acidic alumina as a support, which could also catalyze the isomerization of olefins. This complicates somewhat the comparison with our results, which are free from support effects.

There are a number of possible explanations for the surprising activity enhancement observed for the Au–Pt alloys in our studies.

(a) In our work great care was taken to characterize the surfaces and the observed rate enhancement effects are definitely significant. In the study of the supported Pt–Au system (*24*), the absolute rates were not determined as rates were only determined per unit weight of the catalysts without selective determination of the surface area of the active metal component. One possible explanation for the apparent differences between our work and the literature data is, therefore, that in the latter the active surface areas were overestimated.

(b) In a complex reaction system as with *n*-hexane many reactions occur at the same time and the possibility has to be considered that the effect of alloying operates indirectly by affecting competing side reactions.

Gold was found not only to enhance isomerization, but also dehydrogenation. If 2- and 3-MP are formed from hexene-2, the enhanced olefin formation would cause more isomerization as well. There are, however, two pieces of evidence against this case. First, olefin formation is not only enhanced with the alloys, but also with the epitaxial surfaces. Enhanced isomerization, however, was only pronounced with the alloys. Second, in a separate control experiment on a pure Pt(111) surface, the use of pure hexene-2 instead of *n*-hexane as a reactant did not increase the production of 2- and 3-MP.

Another side reaction that should be considered is the formation of a strongly bound carbonaceous layer on the surface, blocking reaction sites. If the formation of this layer requires large ensembles, this would be suppressed on alloy surfaces where more Pt atoms would be available for reac-

tion than on a largely carbon-covered Pt(111) surface. Unfortunately, the AES measurements of the amounts of carbon deposited by the reaction (Fig. 19) are too scattered to decide this definitively.

(c) The small Pt ensembles may have higher activity than the large Pt ensembles. For the isomerization of pentanes and hexanes high negative reaction orders in hydrogen are found which are currently interpreted by assuming that the rate-determining step is the skeletal rearrangement of highly dehydrogenated species (*26*). When Pt is alloyed with Au the bond strength of the reaction intermediates to the surface may well be less due to the limited number of Pt atoms available in small ensembles. A higher activity of these less strongly bound species could explain the observed isomerization increase.

This argument does not, however, explain the intermediate behavior of MCP in Fig. 15. MCP and 2- and 3-MP may be formed through a common "C_5-cyclic" intermediate and O'Cinneide and Gault have shown that the fraction of isomerization products formed through this intermediate is larger with Pt–Au alloys than with pure Pt (*21b*). With the epitaxial surfaces we found that the initial enhancement of isomerization occurred at the expense of MCP formation. Thus, the intermediate behavior of MCP formation on the surface alloys can be rationalized as a compensation of the enhanced production of intermediates by a decreased selectivity of these species for MCP formation. Consequently the enhanced isomerization would actually be due to the constructive addition of both these effects.

Judging by TPD, the bonding of CO to the Pt–Au alloy and overlayer surfaces is identical to that to the clean Pt(111) surface. The only important effect is the coverage dependence of the heat of adsorption which permitted us to identify the presence of small Pt clusters in the Pt–Au alloy surfaces and of large Pt clusters in the Pt–Au overlayer surfaces. The presence of ligand or electronic effects on the changes of bonding *n*-hexane or certain reaction intermediates that form during the conversion of *n*-hexane to the various products cannot be ruled out, however. The enhancement of the isomerization rate must be due to changes of bonding that are induced either by charge redistribution or by structural changes as small Pt clusters of (111) orientation are produced.

More studies that systematically vary the platinum surface structure and the alloying IB constituent (Cu and Ag instead of Au) are needed to verify the causes of this interesting reaction rate enhancement effect.

5. CONCLUSIONS

(1) Deposition of Au on Pt(111) near 300 K produces an epitaxial Au layer consisting of two-dimensional islands that leave large ensembles of Pt(111) uncovered. With increasing coverage, the islands grow until the monolayer is completed, before the second layer begins to form.

(2) High-temperature annealing of Pt(111) surface covered by several layers of gold produces a surface alloy with small Pt ensembles.

(3) The temperature of the maximum rate of desorption in the TPD spectra of CO is sensitive to the Pt ensemble sizes.

(4) The ligand effect was found to be insignificant for CO adsorption on the Au–Pt(111) alloys.

(5) The alloy surfaces are more active than the corresponding monometallic surfaces with the same Pt content.

(6) The ensemble size has a profound influence on the *n*-hexane skeletal reactions. The small Pt clusters present in the Au–Pt alloys exhibit enhanced isomerization rates and reduced hydrogenolysis and aromatization rates as compared to clean Pt(111) or Pt–Au overlayer surfaces with large Pt clusters.

ACKNOWLEDGMENT

This work was supported by the Director, Office of Energy Research, Office of Basic Energy Sciences,

Materials Sciences Division of the U.S. Department of Energy under Contract DE-AC03-76SF00098.

REFERENCES

1. (*a*) Ponec, V., *Catal. Rev. Sci. Eng.* **11**(1), 41 (1975); (*b*) Clarke, J. K. A., *Chem. Rev.* **75**, 291 (1975); (*c*) Sinfelt, J. H., *Acc. Chem. Res.* **10**, 15 (1977); (*d*) Sachtler, W. M. H., and van Santen, R. A., *in* "Advances in Catalysis and Related Subjects," Vol. 26, p. 69. Academic Press, New York/London, 1977; (*e*) Ponec, V., *Surf. Sci.* **80**, 352 (1979); (*f*) de Jongste, H. C., and Ponec, V., *Bull. Soc. Chim. Belg.* **88**(7–8), 453 (1979).
2. (*a*) Sachtler, W. M. H., *Le Vide* **164**, 67 (1973); (*b*) Ponec, V., and Sachtler, W. M. H., *J. Catal.* **24**, 250 (1972); (*c*) Sinfelt, J. H., Carter, J. L., and Yates, D. J. C., *J. Catal.* **24**, 283 (1972).
3. Soma-Noto, Y., and Sachtler, W. M. H., *J. Catal.* **32**, 315 (1974).
4. (*a*) Stephan, J. J., Ponec, V., and Sachtler, W. M. H., *Surf. Sci.* **47**, 403 (1975); (*b*) Anderson, J. R., Foger, K., and Breakspere, R. J., *J. Catal.* **57**, 458 (1979).
5. Garfunkel, E. L., Crowell, J. E., and Somorjai, G. A., *J. Phys. Chem.* **86**, 310 (1982).
6. Sachtler, J. W. A., Van Hove, M. A., Biberian, J. P., and Somorjai, G. A., *Surf. Sci.* **110**, 19 (1981).
7. Herz, R. K., Gillespie, W. D., Petersen, E. E., and Somorjai, G. A., *J. Catal.* **67**, 371 (1981).
8. Hemminger, J. C., Carr, R., and Somorjai, G. A., *Chem. Phys. Lett.* **57**(1), 100 (1978).
9. Ponec, V., and Sachtler, W. M. H., *in* "Proceedings, 5th International Congress on Catalysis, Palm Beach, 1972" (J. W. Hightower, Ed.), Paper 43, p. 645. North-Holland, Amsterdam, 1973.
10. Rhead, G. E., *J. Vac. Sci. Technol.* **13**(2), 603 (1976).
11. (*a*) Gallon, T. E., *Surf. Sci.* **17**, 486 (1969); (*b*) Jackson, D. C., Gallon, T. E., and Chambers, A., *Surf. Sci.* **36**, 381 (1973).
12. Seah, M. P., *Surf. Sci.* **32**, 703 (1972).
13. Pearson, W. B. (Ed.), "Handbook of Lattice Spacings and Structures of Metals," Vol. 2. Pergamon, London, 1967.
14. Redhead, P. A., *Vacuum* **12**, 203 (1962).
15. Ertl, G., Neumann, M., and Streit, K. M., *Surf. Sci.* **64**, 393 (1977).
16. McCabe, R. W., and Schmidt, L. D., *Surf. Sci.* **66**, 101 (1977).
17. Collins, D. M., and Spicer, W. E., *Surf. Sci.* **69**, 85 (1977).
18. Sachtler, W. M. H., *J. Vac. Sci. Technol.* **9**(2), 828 (1971).
19. (*a*) Froitzheim, H., Hopster, H., Ibach, H., and Lehwald, S., *Appl. Phys.* **13**, 147 (1977); (*b*) Hopster, H., and Ibach, H., *Surf. Sci.* **77**, 109 (1978).
20. Collins, D. M., and Spicer, W. E., *Surf. Sci.* **69**, 85 (1977).
21. (*a*) Gault, F. G., *in* "Advances in Catalysis and Related Subjects," Vol. 30, p. 1. Academic Press, New York/London, 1981; (*b*) O'Cinneide, A., and Gault, F. G., *J. Catal.* **37**, 311 (1975).
22. Biberian, J. P., and Somorjai, G. A., *Appl. Surf. Sci.* **2**, 352 (1979).
23. Davis, S. M., Gordon, B. E., Press, M., and Somorjai, G. A., *J. Vac. Sci. Technol.* **19**(2), 231 (1981).
24. Van Schaik, J. R. H., Dessing, R. P., and Ponec, V., *J. Catal.* **38**, 273 (1957).
25. Sinfelt, J. H., Barnett, A. E., and Dembinski, G. W., U.S. Patent 3,442,973 (1969).
26. Gault, F. G., Amir-Ebrahimi, V., Garin, F., Parayre, P., and Weiseng, F., *Bull. Soc. Chim. Belg.* **88**(7–8), 475 (1979).